J Solid State Electrochem (2009) 13:469–475
DOI 10.1007/s10008-008-0587-2

ORIGINAL PAPER

Optimization of electrochemical aspects for epitaxial depositing nanoscale ZnSe thin films

Xin Zhang · Xuezhao Shi · Chunming Wang

Received: 7 March 2008 / Accepted: 12 May 2008 / Published online: 5 June 2008

Abstract Studies of the electrochemical optimization of ZnSe thin film deposition on polycrystalline Au substrates using electrochemical atomic layer epitaxy are reported. Electrochemical aspects were characterized by means of cyclic voltammetry, differential pulse voltammetry, and coulometry. To study the growth mechanism of the underpotential deposition in the formation of ZnSe, the effects of Zn and Se deposition potentials and a Se-stripping potential were adjusted to optimize the deposition program. The deposit, grown using the optimized program, was proved to be a single-phase ZnSe compound with a strong (220)-preferred orientation by X-ray diffraction analysis, and scanning electronic microscopy observation shows the deposit consisted of nanoscale particles with an average size about 100 nm. The right 1:1 stoichiometric ratio of Zn to Se according to the coulometry suggests that ZnSe is formed.

Keywords ZnSe · EC-ALE · UPD · Electrodeposition · XRD · SEM

Introduction

Zinc selenide, ZnSe, is a II–VI compound semiconductor. Due to its high bandgap (2.67 eV), ZnSe has gained considerable attention in the field of blue emitters and blue lasers [1]. Some of the possible applications for Zinc selenide lie in the blue-green region of the visible spectrum in light-emitting diodes and in photovoltaic laser screens, film transistors, photoelectrochemical cells, etc. [2, 3].

Many experimental techniques such as vacuum evaporation [4], pulsed laser deposition [5], radio frequency magnetron sputtering [6], spray pyrolysis [7], electrodeposition [8, 9], chemical bath deposition [10], chemical vapor deposition [11], molecular beam epitaxy [12], metalorganic vapor phase epitaxy [13], metalorganic chemical vapor deposition [14], and atomic layer epitaxy (ALE) [15] have been employed for preparing zinc selenide thin films.

Electrochemical ALE (EC-ALE), which was put forward by Gregory and Stickney [16], is the electrochemical analog of ALE and atomic layer deposition. It is based on the alternated underpotential deposition (UPD) of the elements that form the compound semiconductor in a cycle. UPD is a surface-limited phenomenon, where an atomic layer of one element is deposited on a second at a potential prior to (under) that needed to deposit the element on itself. Therefore, each deposition cycle forms a monolayer (ML) of the compound, and the number of deposition cycles controls the thickness of deposits. In this way, it is a simple, economical, and viable technique, which produces films of good quality for devices applications. The valuable features of the EC-ALE method are the convenience for producing large-area surfaces, low-temperature growth, and the possibility to control film thickness, morphology, and composition by adjusting the electrical parameters, as well as the composition of the electrolytic solution [17].

A number of II–VI and III–V compound semiconductors have been successfully deposited by EC-ALE [18–22], and work is progressing on the formation of III–VI, IV–VI, and V–VI compounds such as In_2Se_3 [23], SnSe [24], Bi_2Te_3 [25], and Sb_2Te_3 [26].

However, it is quite surprising to realize that ZnSe EC-ALE is far less studied than, for example, cadmium

X. Zhang · X. Shi · C. Wang (✉)
Department of Chemistry, Lanzhou University,
Lanzhou 730000, People's Republic of China
e-mail: wangcm@lzu.edu.cn

chalcogenides [27–29]. There has been a report of ZnSe thin films formed on Ag (111) using EC-ALE in an automated deposition system, by the Foresti group [30]. Films with up to 31 cycles were formed, but the graph of stripping charge suggested that the deposits grew at a rate of only about 0.14 ML per cycle. Thin-layer electrochemical studies of the first 14 cycles of ZnSe growth on polycrystalline Au substrate have been performed by the Stickney group [31], but this group has thus far formed no thicker films using the automated flow-cell deposition system. We have attained no thicker films even more than seven cycles with the initial set of conditions by Stickney et al. for ZnSe deposition on a Au substrate. In addition, no structural data can be exhibited in the other literatures available to confirm their experimental results and elucidate the morphological structures of ZnSe formed by EC-ALE.

This paper presents electrochemical optimization studies of ZnSe deposition by EC-ALE to produces homogeneous and stoichiometric deposits. A detailed analysis of the growth mechanism of Se and Zn on the Au substrate was carried out to find the cause of low coverage or growth breaking in electrochemical epitaxial process of previous literatures. In this work, the growth of ZnSe films is continuous, and the rate is not as low as previous literatures. Thus, the deposits are ideal and stoichiometric, and structural analyses and surface morphological of the deposits by electrochemical epitaxy can be reported for the first time.

Materials and methods

The electrochemical cell used for these studies consists of a three-electrode system and a CHI 660 electrochemical workstation (CH Instrument, USA). The auxiliary electrode was a platinum foil, and the reference electrode was a Ag/AgCl (in saturated KCl) electrode. The substrate was a CHI 101 gold disk electrode. Its exposed surface was polished to a mirror finish with 0.5-μm alumina and cleaned ultrasonically in twice-distilled water for about 5 min. Before experiments, an electrochemical cleaning was performed with cyclic voltammetry (CV) in fresh 1 M H_2SO_4 from 0.4 to −1.3 V to assure surface cleanliness.

Experimental coverages in this paper are reported as the ratio of deposited atoms per substrate surface atom. A 3.14-mm^2 geometric surface area was determined, and the polycrystalline electrode can be assumed here as an average of some low index planes.

All Zn solutions consisted of 2.5 mM $ZnSO_4$ with a 0.5-M NH_4Ac solution as the supporting electrolyte, and the pH value was adjusted with ammonium hydroxide to 9. Se solutions consisted of 2.5 mM H_2SeO_3 with a 0.5-M Na_2SO_4 solution as supporting electrolyte, and the pH value was 4. The blank solution contained only 0.5 M Na_2SO_4, at pH 4. Water used for solutions was purified by the Milli-Q system (Millipore, nominal resistivity 18.2 MΩ cm^{-1}), and the chemicals were reagent grade or better. Prior to each experiment, all the solutions were carefully deaerated by blowing purified N_2.

Optimal deposition conditions were studied and characterized electrochemically using CV, differential pulse voltammetry, and coulometry. The crystallographic structures of the thin films obtained were determined by an X-ray diffractometer (XRD, Rigaku D/max-2400), and the morphologies are investigated by scanning electronic microscopy (SEM, Kevex JSM-5600LV).

Results and discussion

Formation of Se atomic layers on Au

A detailed analysis of Se (IV) electroreduction on the Au substrate is in progress in our laboratory by means of CV. Figure 1a shows the cyclic voltammograms of Se electrodeposited from a 2.5 mM H_2SeO_3+0.5 M Na_2SO_4 solution onto the Au substrate, successively scanned from 1.00 V to different cathodic potential limits (0.10, −0.10, −0.20, and −0.30 V, respectively). There are only the first submonolayer reduction peak C1 (at 0.19 V) and its little stripping peak A1 (at 0.72 V) in the solid curve, corresponding to a cathodic scan limit of 0.1 V. While scanned negatively to −0.10 V (dash curve in Fig. 1a), the second reduction peak C2 appeared, and its stripping peak A2 became higher and higher with the electrode scanned negatively to −0.20 and −0.30 V. Based upon the four electrons process for Se reduction shown in reaction 1, the coverages for the reductive peaks C1 and C2 (in dotted curve in Fig. 1a) were calculated as 0.62 and 2.91 ML, as expected for UPD and bulk deposition, a ML in this case refers to an elemental atom layer relative to the number of Au substrate surface atoms, and a ratio of 1.0 refers to a full ML.

$$H_2SeO_3 + 4H^+ + 4e^- \leftrightarrow Se + 3H_2O \quad (1)$$

As the potential was scanned negative of −0.30 V, another cathodic peak C3 (at −0.49 V) and a new oxidative voltammetric feature A3 (at 0.84 V) were observed. Furthermore, A2, the oxidation peak of bulk Se, grew lower and lower as the negative limit for the scan decreased. Similar to most literatures, the peak C3 should be corresponded to bulk Se (0) reduction to Se^{2-}, as reaction 2 shows. Thus, A2 is much smaller with the reductive stripping of bulk Se deposit.

$$Se + 2H^+ \leftrightarrow H_2Se \quad (2)$$

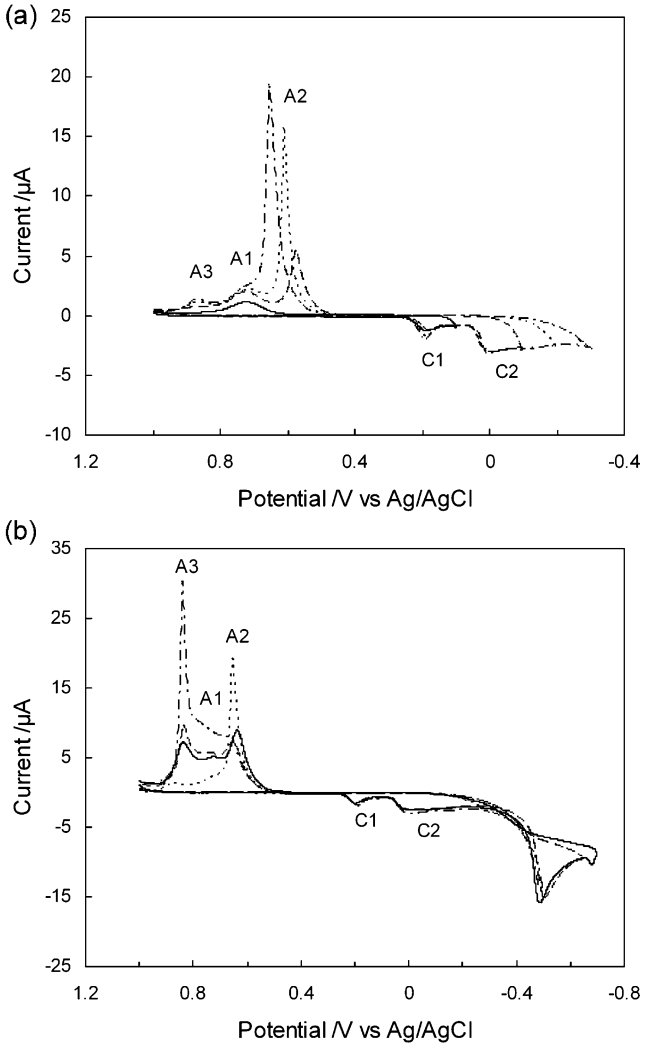

Fig. 1 Cyclic voltammograms of Au electrode in 2.5 mM H_2SeO_3 with a 0.5-M Na_2SO_4 solution, pH 4. The cathodic potential limits were **a** 0.10, −0.10, −0.20, and −0.30 V; (**b**) −0.30, −0.50, and −0.70 V, respectively (scan rate=10 mV/s)

However, it is interesting to note that A3 grew higher until it reached a limiting value (dash-dotted curve in Fig. 1b), then gradually decreased again. According to the literature [32], the reduction of bulk Se to Se^{2-} will be accompanied with a conproportionation reaction, which is also named a subsequent homogeneous chemical reaction, as reaction 3 shows.

$$H_2SeO_3 + 2H_2Se \leftrightarrow 3Se + H_2O \quad (3)$$

Red Se was produced by the conproportionation or subsequent homogeneous chemical reaction, which could be reduced further with the potential scanned toward more negative values. Therefore, the last reductive peak observed beginning at about −0.65 V, which labeled C4 in the voltammogram, corresponds to the reduction of red Se. Thus, the appearance of peak A3 may be attributed to the oxidative stripping of red Se formed by reaction 2 from the Se^{2-} ions, and its decrease was due to the second reduction in red Se. Further scanning in the cathodic direction resulted in hydrogen evolution below −0.80 V.

Formation of Zn atomic layers

Zn is underpotentially deposited both on Au and on a Se-covered Au electrode. Figure 2a shows the voltammogram of Zn^{2+} on the Au substrate. The UPD Zn was observed on polycrystalline Au in an ammonia buffer solution, associated with peaks C1 at −0.14 V and A1 in approximately 0 V, while bulk Zn deposition was found to occur only at potentials more negative than −0.5 V, associated with peaks C2, A3, and A2. The Zn UPD has been extensively studied by Igarashi et al. [33].

The voltammograms of a Se-covered Au electrode in the 0.5 M NH_4Ac and in 2.5 mM $ZnSO_4$+0.5 M NH_4Ac, pH 9, solutions are shown in Fig. 2b. In these experiments, the potential scanning was started at 0.20 V in the cathodic direction to avoid the oxidative stripping of Se. In the absence of Zn^{2+}, there were two stripping peaks on the

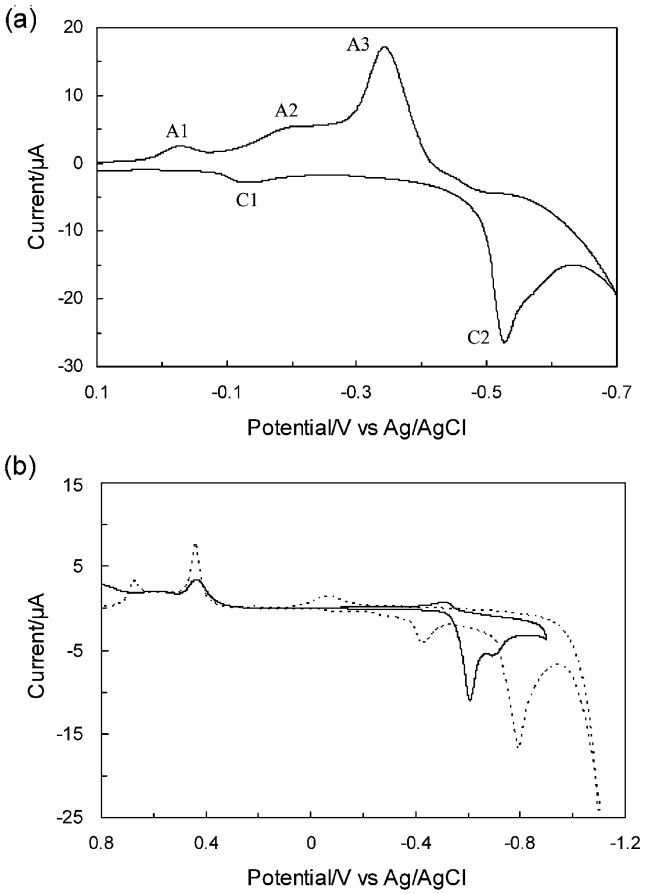

Fig. 2 Cyclic voltammograms of **a** the bare Au electrode in 2.5 mM $ZnSO_4$ with a pH 9 ammonia buffer solution; **b** Se-covered Au electrode in 0.5 M ammonia buffer blank solution, pH 9 (*solid curve*), and 2.5 mM $ZnSO_4$ with a pH 9 ammonia buffer solution (*dashed curve*). The scan rate is 10 mV/s

cathodic scan (solid curve in Fig. 2b), respectively, corresponding to the reduction of bulk Se at −0.61 V and red Se started at −0.65 V. However, there was no apparent stripping peak of Se but another peak at a potential of −0.45 V corresponding to Zn UPD, observed for the voltammetry curve of Zn on a Se-covered Au electrode (dotted curve). In this case, dissolution of Se from the electrode surface through oxidative stripping occurs between 0.40 and 0.80 V yet. Therefore, depositing Zn at −0.45 V would restrain deposited Se from reductive stripping as reaction 4. The corresponding stripping feature for UPD Zn occurred at −0.05 V.

$$Zn^{2+} + H_2Se \leftrightarrow ZnSe + 2H^+ \quad (4)$$

In fact, the most important requirement for an EC-ALE cycle is that the deposition of one element should not destroy the underlying layer of the other element. It is obvious that the dissolution of the deposited Zn does not occur at potentials negative to −0.20 V for Se UPD; thus, −0.20 V could be applied for the deposition of a further Se layer on a Au/Se/Zn substrate.

Mechanism of ZnSe formation

The potential of 0.20 V for Se was identified as reasonable initial potentials for the EC-ALE cycle. However, the reductive stripping current of Se, deposited at a constant deposition potential of 0.20 V, increases with the accumulation time, and the charges measured in the reductive stripping of the deposited Se appears to be a linear function of the deposition time (Fig. 3). The surface-limited process is fast, reaching completion quickly, while the bulk deposition is slow, resulting in a small steady-state current [34]. The amount of bulk Se deposit depends on the deposition time. Thus, the linear dependence suggests the formation of some bulk Se on the surface at 0.20 V. The probable explanation for the bulk deposition is Se does not result in a classic UPD process. On the contrary, Se deposition requires an overpotential [35].

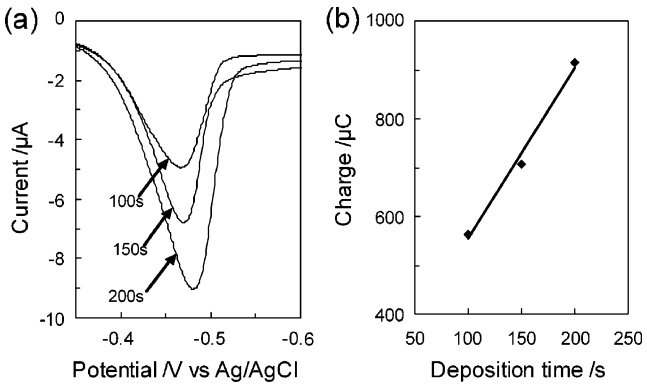

Fig. 3 Cyclic voltammograms for the reductive stripping of Se deposited at 0.20 V on Au substrate (scan rate=10 mV/s). The three curves refer to deposition times of 100, 150, and 200 s (**a**). **b** The corresponding plots of the charge involved in the reductive stripping of Se in **a**

The bulk Se can be removed by the introduction of an extra step designed to reduce excess bulk Se to a soluble selenide species, previously suggested by this paper. After 15 s of Se deposition, the cell was rinsed with blank solution for 5 s, at which point the potential was shifted negatively, such that bulk Se was reduced to HSe^-. HSe^- is a soluble species, which diffuses away, leaving only UPD Se on the surface.

According to the previous literature, potentials at which point bulk Se was reductive stripping were often set for Se deposition and stripping simply. For instance, −0.50 V was set as potentials for both deposition and reductive stripping [31]. Based on the previous CV studies of Se in this paper, however, a large amount of bulk and red Se was produced by the conproportionation reaction, which was loose and porous [32], and reduced the interaction between Zn and UPD Se. Moreover, in the process of Zn electrodeposition, the anion will react with the underlying Se layer through micropores of red Se and induce its stripping, which would seriously inhibit the UPD of Zn, followed by the increase in difficulty and complexity of nucleation.

The kinetics of ML formation by two dimensional nucleation and growth is now well understood [36]: Current density–time transients are described by the equations

$$j_{inst} = at\exp\left(-bt^2\right) \quad (5)$$

for the instantaneous case and

$$j_{prog} = ct^2\exp\left(-dt^3\right) \quad (6)$$

for the progressive case. ZnSe is an *n*-type semiconducting material, which accord with the latter case. We fit the experimental current–time data of one EC-ALE cycle (Se at −0.20 V, Zn at −0.45 V) to the progressive case, which indeed indicated the low rate of the deposition of ZnSe ML. Plus the effect of red Se, It is very difficult for the Zn UPD on Se. Thus, in the previous work, ZnSe was hardly formed by EC-ALE, or the coverages of deposits were quite low.

Therefore, how to avoid the formation of red Se is the main problem in this work. The suggested procedure to obtain an UPD layer of selenium consists in depositing an excess of selenium at −0.20 V and then applying a potential of −0.70 V, which is picked as the reductive stripping potential for the bulk Se and red Se formed from the subsequent conproportionation.

EC-ALE cycles

The preliminary EC-ALE cycle designed to deposit ZnSe appeared to be as follows: The Se solution was filled into the

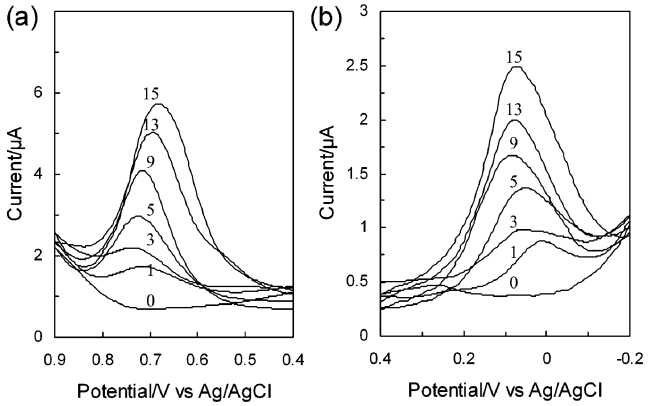

Fig. 4 Cyclic voltammograms of Se layers (**a**) and Zn layers (**b**) from 1, 3, 5, 9, 13, and 15 cycle deposits. The scan rate is 10 mV/s

cell and held static for 15 s at −0.20 V. The cell was then flushed with the blank solution, and the potential was changed to −0.70 V for 5 s. After this, the Zn solution was filled and deposited for 15 s at −0.50 V. To avoid codeposition of ZnSe, a blank rinse was used before the introduction of each solution, and this cycle was repeated as many times as desired.

The deposition charges, however, decreased over the first few cycles, and almost no thicker deposit is formed after five cycles. This may be attributed to the contact resistance between the predeposits and the metallic electrode, which consumes a part of the potential. In the initial stage of EC-ALE, atomic layers grow heteroepitaxially on the Au electrode. As the semiconductor films grow, especially over the first ten cycles, the contact resistance varies gradually with the structure of the deposit evolving into normal ZnSe structure from initial mismatch with the Au lattice. Therefore, the depositing potentials for Zn and Se should be adjusted negatively until the steady-state conditions were reached. Similar potential adjusting was also adopted in the first 10–30 cycles for most of the

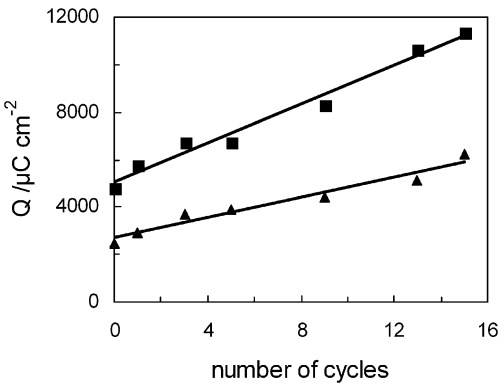

Fig. 5 Plots of the charge involved in the stripping of Se (*squares*) and Zn (*triangles*) as a function of the number of EC-ALE cycles. The slopes yield 400.11 μC cm^{-2} per Se layer and 201.88 μC cm^{-2} per Zn layer

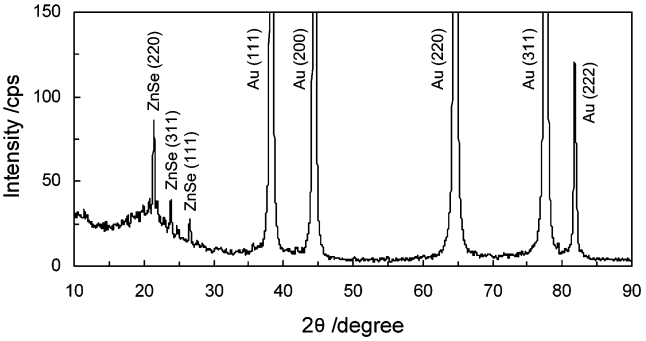

Fig. 6 X-ray diffraction of a seven-cycle electrodeposited ZnSe thin film. The angle of incidence is 1°, Cu Kα source

compounds formed via EC-ALE [23, 37], to maintain reasonable quality deposits.

In this work, the deposition potentials were negatively adjusted in the first deposition stage, according to the response current and depositing charge, until steady-state potentials of −0.59 V for Se and −0.86 V for Zn were

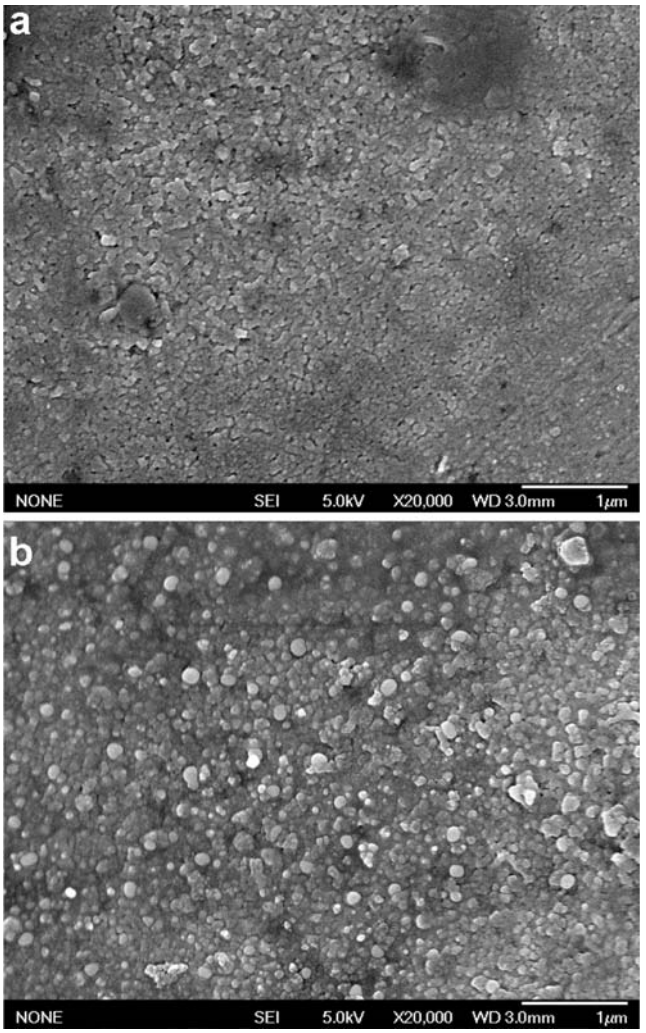

Fig. 7 SEM micrographs of the Au substrate and ZnSe deposits. **a** Au substrate and **b** ZnSe deposits

attained. Thus, the optimal EC-ALE cycle for ZnSe deposition consisted of Se deposition at −0.20 V in the Se solution, followed by reductive dissolution of the excess Se to selenide at −0.70 V in the blank solution to leave a Se atomic layer, and finally Zn UPD at −0.50 V, in the Zn solution to complete the deposition cycle. The potentials for deposition were stepped negative after each of the first 15–20 cycles, until steady-state potentials of −0.59 V for Se and −0.86 V for Zn were attained. Repeat this cycle as many times as desired to grow nanofilms of ZnSe on Au substrate.

Characterization of ZnSe thin film

Limiting the number of cycles used in creating 15 alternate layers of Se and Zn as a maximum is justified by the lengthy operations carried out manually. Once the deposit was formed, the amount of elements deposited in a given number of cycles was estimated from the charge involved in their stripping. The overall charges involved in stripping deposits formed with a different number of cycles was determined by oxidative stripping of Zn from −0.2 to 0.4 V and Se from 0.4 to 0.9 V.

Figure 4a,b shows the oxidative stripping peaks of 1–15 Se layers (a) and the corresponding Zn layers (b) carried out in a blank solution, and Fig. 5 shows plots of the charges for Zn and Se stripping as a function of the number of cycles. In Fig. 4a,b, "0 cycle" refers to the stripping voltammograms of the bare Au electrode as a blank sample, which still has a certain current density in the stripping solution. The plots are linear, and the charges involved in the stripping voltammograms of the blank sample are approximately equal to the values at which point the extrapolated linear plots intercept *y*-axis. With the deduction of the blank value, an average charge per cycle of 400.11 μC cm^{-2} for Se and 201.88 μC cm^{-2} for Zn was calculated.

For better investigation of the morphology and structure of the deposited films, a seven-cycle deposit was prepared on a plane gold electrode instead of a CHI disk electrode. Its XRD pattern is shown in Fig. 6. Peaks corresponding to (111), (220), and (311) planes of ZnSe were evident, and no elemental peaks for Zn and Se were observed, suggesting that the deposit was a single-phase ZnSe compound with a strongly predominant (220) orientation, not the mixture of elemental Zn and Se.

The morphology of ZnSe deposits, along with the Au substrate, was observed with SEM and shown in Fig. 7. Au substrate before deposition is shown in Fig. 7a, and the SEM image of the deposits is shown in Fig. 7b. The surface morphology of the deposit consists of many small ZnSe particles with uniform grain size about 100 nm in diameter. The grains are packed very closely and shown as homogeneous granules.

Conclusions

The linear behavior of plots in Fig. 5 supports layer-by-layer growth. The charges of 400.11 and 201.88 μC cm^{-2} associated with each layer of Se and Zn correspond to the ideal coverage of 0.562 and 0.567 ML and prove to be an almost stoichiometric ratio between the elements, as expected for the formation of the ZnSe compound. XRD analysis and SEM observation demonstrate that the EC-ALE methodology is applicable to the deposition of the high-quality nanodeposit of stoichiometric ZnSe on Au substrates using EC-ALE, if the deposition condition has been optimized.

Future work will be devoted to an investigation of the morphology and structure of thin ZnSe films formed on single-crystalline substrates by a higher number of cycles. This higher number of cycles can be obtained only with an automated system, whose setup is in progress in our laboratory.

Acknowledgments The authors acknowledge the support of the Special Doctoral Foundation of the Ministry Education of China (Grant no. 20030730014.1).

References

1. Morkoc H, Strite S, Gao GB, Lin ME, Sverdlov B, Burns M (1994) J Appl Phys 76:1363
2. Drechsler M, Meyer BK, Hofmann DM, Ruppert P, Hommel D (1997) Appl Phys Lett 71:1116
3. Ennaoui A, Siebentritt S, Lux-Steiner MC, Riedl W, Karg F (2001) Sol Energy Mater Sol Cells 67:31
4. Sherif ME, Terra FS, Khodier SA (1996) J Mater Sci Mater Electron 7:391
5. Xue MZ, Fu ZW (2006) Electrochim Acta 52:988
6. Rizzo A, Tagliente MA, Caneve L, Scaglione S (2000) Thin Solid Films 368:8
7. Bedir M, Öztaş M, Bakkaloğlu ÖF, Ormanci R (2005) Euro Phys J B 45:465
8. Riveros G, Gomez H, Henriquez R, Schrebler R, Marotti RE, Dalchiele EA (2001) Sol Energy Mater Sol Cells 70:255
9. Machado SAS, Manzoli A, Santos MC (2007) Thin Solid Films 515:6860
10. Lokhande CD, Patil PS, Ennaoui A, Tributsch H (1998) Appl Surf Sci 123–124:294
11. Rumberg A, Sommerhalter C, Toplak M, Jager-Waldau A, Lux-Steiner MC (2000) Thin Solid Films 361–362:172
12. Tamargo MC, Nahory RE, Skromme BJ, Shibli SM, Weaver AL, Martin RJ, Farrell HH (1991) J Cryst Growth 111:741
13. Chergui A, Samah M, Bouguerra M, Guerbous L (2006) Mater Sci Eng B 131:177
14. Skromme BJ, Liu W, Jensen KF, Giapis KP (1994) J Cryst Growth 138:338
15. Godlewski M, Guziewicz E, Kopalko K, Lusakowska E, Dynowska E, Godlewski MM, Goldys EM, Phillips MR (2003) J Lumin 102–103:455
16. Gregory BW, Stickney JL (1991) J Electroanal Chem 300:543
17. Innocenti M, Pezzatini G, Forni F, Foresti ML (2001) J Electrochem Soc 148:C357

18. Colletti LP, Flowers BH Jr, Stickney JL (1998) J Electrochem Soc 145:1442
19. Innocenti M, Forni F, Pezzatini G, Raiteri R, Loglio F, Foresti ML (2001) J Electroanal Chem 514:75
20. Flowers BH, Wade TL, Garvey JW, Lay M, Happek U, Stickney JL (2002) J Electroanal Chem 524–525:273
21. Wade TL, Ward LC, Maddox CB, Happek U, Stickney JL (1999) Electrochem Solid State Lett 2:616
22. Wade TL, Vaidyanathan R, Happek U, Stickney JL (2001) J Electroanal Chem 500:322
23. Vaidyanathan R, Stickney JL, Cox SM, Compton SP, Happek U (2003) J Electroanal Chem 559:55
24. Qiao Z, Shang W, Wang C (2005) J Electroanal Chem 576:171
25. Zhu W, Yang JY, Hou J, Gao XH, Bao SQ, Fan XA (2005) J Electroanal Chem 585:83
26. Yang JY, Zhu W, Gao XH, Bao SQ, Fan X, Duan XK, Hou J (2006) J Phys Chem B 110:4599
27. Muthuvel M, Stickney JL (2006) Langmuir 22:5504
28. Loglio F, Innocenti M, D'Acapito F, Felici R, Pezzatini G, Salvietti E, Foresti ML (2005) J Electroanal Chem 575:161
29. Foresti ML, Pozzi A, Innocenti M, Pezzatini G, Loglio F, Salvietti E, Giusti A, D'Anca F, Felici R, Borgatti F (2006) Electrochim Acta 51:5532
30. Pezzatini G, Caporali S, Innocenti M, Foresti ML (1999) J Electroanal Chem 475:164
31. Colletti LP, Thomas S, Wilmer E, Stickney JL (1997) Mater Res Soc Symp Proc 451:235
32. Espinosa AM, Tascon ML, Vazquez MD, Batanero PS (1992) Electrochim Acta 37:1165
33. Igarashi K, Aramata A, Taguchi S (2001) Electrochim Acta 46:1773
34. Lister TE, Stickney JL (1996) Appl Surf Sci 107:153
35. Huang BM, Lister TE, Stickney JL (1997) Surf Sci 392:27
36. Bhattacharjee B, Rangarajan SK (1991) J Electroanal Chem 302:207
37. Vaidyanathan R, Stickney JL, Happek U (2004) Electrochim Acta 49:1321